AN EXERGY ANALYSIS FOR OVERALL HIDDEN LOSSES OF ENERGY IN SOLAR WATER HEATER

by

Sathyakala PONNUSAMY[a*], Sai Sundara Krishnan GANGADHARAN[b], and Balaji KALAIARASU[c]

[a] Department of Mathematics, PSG College of Technology, Tamilnadu, India
[b] Department of Applied Mathematics and Computational Sciences, PSG College of Technology, Tamilnadu, India
[c] Department of Mechanical Engineering, Amrita School of Engineering, Ettimadai, Tamilnadu, India

Original scientific paper
https://doi.org/10.2298/TSCI200530343P

This study investigates the hidden thermal losses of glass plate, collector plate, water pipe and storage tank of solar water heater in the process of energy conversion. The present non-conventional energy methods are insufficient, whereas the exergy analysis provides a remarkable solution. Thus, employing the exergy analysis, entropy generation, exergy destruction, and exergy efficiency of each subsystem of solar water heater are computed. The obtained results showed that the entropy generation and exergy destruction are high during the heat transfer in each subsystem. Henceforth, the existing solar water heater design is modified placing hexagonal honeycomb structure between the glass plate and the collector plate and also water pipe is insulated to trap huge amount of solar energy. The proposed design exhibits improved exergy efficiency when compared with the existing model, which enhances the performance of the system.

Key words*: solar water heater, energy balance, exergy destruction, exergy efficiency*

Introduction

The world energy demand is rapidly rising due to the high speed growing of technology. The increased depletion of fossil fuels has led to the quest for alternative fuel resources of energy. Currently, solar energy is the most accessible and inexhaustible form of energy, which involves considerable attention for generating heat and electricity. Solar water heater (SWH) is the popular source of solar energy utilization because of technological feasibility and economic attraction, when compared to other kinds of solar energy utilization. Thus, to optimize solar system design parameters and process, the Second law of thermodynamics (exergy efficiency) is necessary [1].

Suzuki [1] a compared an evacuated tubular collector and a flat-plate collector by assuming a fixed overall heat loss coefficient, and showed that they both have nearly equal potential in exergy gain. Gupta *et al.* [2] carried out a thermal and exergy investigation of solar collector by assuming an invariable overall heat loss coefficient and fluid inlet temperature. Luminosu and Fara [3] proved that the collector's overall exergy efficiency depends upon flu-

* Corresponding author, e-mail: psl.maths@psgtech.ac.in

id-flow rate plus the collector area. Farahat *et al.* [4] had developed an exergetic optimization of a flat plate solar collector, to determine the optimal performance and design parameters of the solar to a thermal energy conversion system.

Jafarkazemi *et al*. [5] showed experimentally and theoretically, better exergetic performance as an effect of rising water inlet temperature along with decreasing water mass-flow rate. Zhong *et al.* [6] had proposed exergy model for the study of flat plate solar collectors by taking into account a non-uniformity in the temperature distribution along the absorber plate. Sivaraman *et al*. [7] proposed that the flat plate bend tube solar collector employs additional energy which in turn enhances the outlet water temperature. Malvi *et al.* [8] experimentally pointed out the heat removal factor, F_R, is highly influenced by the systems fin efficiency and its value does not increases for the mass-flow rate beyond 4 kg per hour. Orlando *et al.* [9] showed that the heat removal factor, F_R, linearly increases with 14.5% change for inclinations from horizontal to vertical.

Hollands [10] presented a simplified analysis of four aspects of squared honeycomb array and pointed the significance of wall thickness of honeycomb. Mozumder *et al.* [11] found the performance of the system with the honeycomb is enhanced than the one without the honeycomb when the incident angle of the solar radiation is within 20°. Abdullah *et al.* [12] revealed the use of honeycomb in solar collectors has a benefit of reducing the top heat loss and also the penalty of decreasing the optical efficiency.

The previous studies recognized the importance of utilization of renewable energy in SWH, optimization of flat plate collector efficiency, energy conversion and exergy analysis. This motivated the present study to focus on the experimental work to extract hidden losses by accounting exergy destruction in each subsystem of the SWH using the Second law of thermodynamics.

Thermodynamic analysis of solar water heater

The energy, exergy and entropy [13] for each subsystem of the SWH are analyzed by considering the output at each stage as input for the subsequent stages with the assumptions:

- all of the correlations have been written in 1-D steady-state and steady flow condition,
- iterative procedure is employed to estimate the top loss coefficient with the range of variables as shown in tab. 1,
- the solar collector's heat transfer coefficient and agent fluid properties are taken as constants, and
- the exergy loss caused by the ducts' pressure drop is negligible.

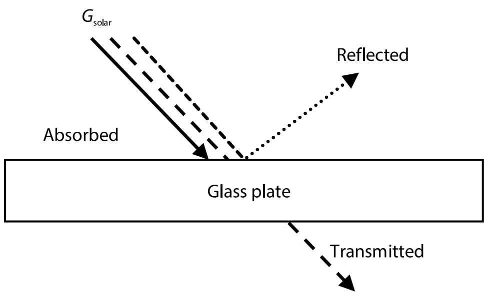

Figure 1. Glass plate

Glass plate

The glass plate [11] in fig. 1 reduces convective and radiative heat losses from the absorber, to transmit incident solar radiation the absorber plate with minimum loss and to protect the absorber plate from the effects of climatic change.

Energy absorption

The heat energy input rate in the glass plate from the solar energy:

$$\dot{Q}_{\text{in,gp}} = \alpha_{\text{s}} G_{\text{solar}} A_{\text{p}} \tag{1}$$

Heat transfer loss rate from the glass plate occurs in two modes, namely radiation and convection and is given:

$$\dot{Q}_{l,\mathrm{gp}} = \varepsilon\sigma A_\mathrm{p}\left(T_\mathrm{sf}^4 - T_\mathrm{air}^4\right) + h_\mathrm{conv} A_\mathrm{p}\left(T_\mathrm{sf} - T_\mathrm{air}\right) \tag{2}$$

The convective heat transfer coefficient is calculated based on the correlation between Rayleigh, Ra_L, and Nusselt number, Nu_L. The rate of heat energy absorbed by the glass plate:

$$\dot{Q}_\mathrm{abs,gp} = \dot{Q}_\mathrm{in,gp} - \dot{Q}_{l,\mathrm{gp}} \tag{3}$$

The heat energy absorbed by the glass plate will be the input for the honeycomb structure.

Entropy generation

The increase of entropy principle states that the entropy can only be created. At steady-state, entropy change is zero. The rate of entropy generation within the glass plate is calculated:

$$\dot{S}_\mathrm{gen,gp} = \frac{\dot{Q}_{l,\mathrm{gp}}}{T_\mathrm{air}} \tag{4}$$

Exergy destruction and exergy efficiency

The loss of available energy due to the conception of entropy in irreversible processes of the glass plate is articulated by exergy. The exergy destruction of the glass plate:

$$\dot{X}_\mathrm{des,gp} = T_\mathrm{o}\dot{S}_\mathrm{gen,gp} \tag{5}$$

$$\eta_\mathrm{ex,gp} = 1 - \frac{\dot{X}_\mathrm{des,gp}}{\dot{X}_\mathrm{in,gp}} \tag{6}$$

Honeycomb structure

Each subsystem of the SWH is analyzed to determine the areas of major heat losses. Although, solar collector transfers the solar energy into useful heat in a competent way, the efficiency of solar collector is low due to heat dissipation. To reduce the exergy destruction two modifications to the design were adapted specifically, honeycomb structure, and water pipe insulation. The heat loss by radiation forms an essential fraction of total heat loss from the top surface of the absorber plate. A honeycomb layer is sited between the collector and glass cover plate which acts as convection suppression device that reduces the heat loss and increases the collector's efficiency.

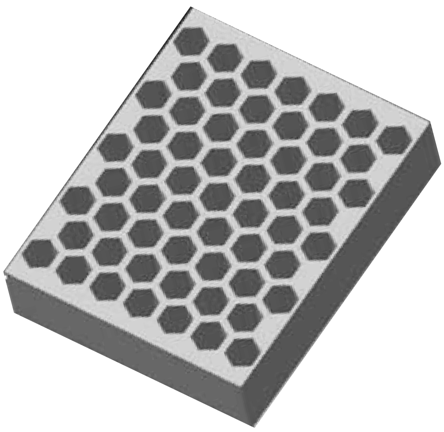

Figure 2. The 3-D view of honeycomb structure

Energy absorption

The energy balance for honeycomb structure is given:

$$\dot{Q}_\mathrm{in,hc} - \dot{Q}_{l,\mathrm{hc}} = \dot{Q}_\mathrm{out/abs,hc} \tag{7}$$

where $\dot{Q}_{\text{in,hc}} = \dot{Q}_{\text{abs,gp}}$, as the output of previous stage is considered as input of present stage. Heat transfer loss from the honeycomb devices occur in three forms, namely natural-convection, radiation and conduction heat transfer through honeycomb walls. The conventional heat loss:

$$\dot{Q}_{l,\text{hc}} = U_{\text{hc}} A_{\text{p}} \left(T_{1=,\text{hc}} - T_{2,\text{hc}} \right) \tag{8}$$

where $T_{1,\text{hc}}$, $T_{2,\text{hc}}$ are temperature differences of two faces of honeycomb panel.

The overall heat transfer coefficients U_{hc} across the panel is given:

$$U_{\text{hc}} = h_{\text{a}} + h_{\text{r}} + h_{\text{c}} \tag{9}$$

The natural heat transfer coefficient h_{a}, based on Nusselt number:

$$h_{\text{a}} = \frac{\text{Nu}_L K_{\text{a}}}{d} \tag{10}$$

Also, if the faces of the honeycomb are grey and have emissivity's ε_1 and ε_2 and reflectance's ρ_1 and ρ_2, the radiant heat flux h_{r} between the two faces [14]:

$$h_{\text{r}} = \frac{F_1 \sigma \left(T_{1,\text{hc}}^4 - T_{2,\text{hc}}^4 \right)}{\left(T_{1,\text{hc}} - T_{2,\text{hc}} \right)} \tag{11}$$

$$\frac{1}{F_1} = \frac{1}{F} + \frac{\rho_1}{\varepsilon_1} + \frac{\rho_2}{\varepsilon_2} \tag{12}$$

where F, F_1 are the equivalent form factors between the two faces [14]. Then the mean heat flux h_{c} for hexagonal array in fig. 2 might be is defined:

$$h_{\text{c}} = \frac{3\delta K_H \left(T_1 - T_2 \right)}{wd} \tag{13}$$

Figure 3. Experimental set-up

Flat collector plate

A flat plate solar collector in fig. 3 carries out the three effective mechanisms:

– absorbs the utmost potential amount of solar irradiance,
– conduct heat in the direction of the working fluid at least temperature difference, and
– drop smallest amount of heat back to the surroundings.

Energy absorption

The useful heat gain by the working fluid:

$$\dot{Q}_{\text{cp}} = \dot{m} C_p \left(T_{\text{out,cp}} - T_{\text{in,cp}} \right) \tag{14}$$

There is no mass-flow in the absorber plate under steady-state. Also, the heat energy absorbed by the honeycomb panel will be the input for the collector plate. By considering, overall heat loss coefficient U_l, the Hottel-Whillier equation for useful heat collected per unit area [15] is:

$$\dot{Q}_{\text{cp}} = A_{\text{p}} F_R \left[S_{\text{r}} - U_l \left(T_{\text{in}} - T_{\text{air}} \right) \right] \tag{15}$$

Based on the three components, the top loss coefficient U_t, the bottom loss coefficient U_b, and the side loss coefficient U_s, U_l given:

$$U_l = U_t + U_b + U_s \tag{16}$$

The heat removal factor is defined:

$$F_R = \frac{\dot{m}C_p}{U_l A_p}\left[1-\exp\left\{\frac{F'U_l A_p}{\dot{m}C_p}\right\}\right] \tag{17}$$

In eq. (15), the radiation absorbed flux by unit area of the absorber plate is defined:

$$S_r = (\tau\alpha) I_T \tag{18}$$

Entropy generation

The rate of change of the entropy generated in the collector plate is given:

$$\dot{S}_{gen,cp} = \frac{\dot{Q}_{l,cp}}{T_{air}} \tag{19}$$

The heat loss from the collector plate in terms of overall loss coefficient is expressed:

$$\dot{Q}_{l,cp} = U_l A_p \left(T_p - T_{air}\right) \tag{20}$$

Exergy destruction and exergy efficiency

The general form of exergy balance of the collector plate:

$$\dot{X}_{in} + \dot{X}_{sd} + \dot{X}_{out} + \dot{X}_{lk} + \dot{X}_{des} = 0 \tag{21}$$

where $\dot{X}_{in}$, $\dot{X}_{sd}$, $\dot{X}_{out}$, $\dot{X}_{lk}$, and $\dot{X}_{des}$ are the inlet, stored, outlet, leakage, and destroyed exergy rate, respectively. The inlet exergy rate includes the inlet exergy rate with fluid-flow and the absorbed solar radiation exergy rate. The inlet exergy rate with fluid-flow:

$$\dot{X}_{in,m} = \dot{m}C_p\left[T_{in,cp} - T_{air} - T_{air}\ln\left(\frac{T_{in,cp}}{T_{air}}\right)\right] \tag{22}$$

Assuming the sun as an infinite thermal source, the absorbed solar radiation exergy rate [16]:

$$\dot{X}_{in,r} = \eta_o I_T A_p\left(1-\frac{T_{air}}{T_{Sun}}\right) \tag{23}$$

The summing up of eqs. (22) and (23) will result in total inlet exergy rate of the solar collector. The stored exergy rate is null at steady-state conditions. The outlet exergy rate includes only the exergy rate of outlet fluid-flow.

$$\dot{X}_{out,m} = -\dot{m}C_p\left[T_{out,cp} - T_{air} - T_{air}\ln\left(\frac{T_{out,cp}}{T_{air}}\right)\right] \tag{24}$$

The leakage exergy rate caused by heat leakage rate from the absorber plate to the environment [2]:

$$\dot{X}_{\text{lk}} = -U_l A_{\text{p}} \left(T_{\text{p}} - T_{\text{air}}\right)\left(1 - \frac{T_{\text{air}}}{T_{\text{p}}}\right) \tag{25}$$

The destroyed exergy rate comprises two expressions: the first is caused by the temperature difference between the absorber plate surface and the Sun [2], the second is caused by the temperature difference between the absorber plate surface and the agent fluid [1]. Correspondingly the equations are

$$\dot{X}_{\text{des},\Delta T_{\text{s}}} = -\eta_o I_T A_{\text{p}} T_{\text{air}} \left(\frac{1}{T_{\text{p}}} - \frac{1}{T_{\text{Sun}}}\right) \tag{26}$$

$$\dot{X}_{\text{des},\Delta T_f} = -\dot{m} C_p T_{\text{air}} \left[\ln\left(\frac{T_{\text{out,cp}}}{T_{\text{in,cp}}}\right) - \left(\frac{T_{\text{out,cp}} - T_{\text{in,cp}}}{T_{\text{p}}}\right)\right] \tag{27}$$

Substituting eqs. (22)-(27) into eq. (21) and considering the exergy efficiency definition, the Second law efficiency is derived [2, 3, 16]:

$$\eta_{\text{ex,cp}} = 1 - \left\{ \left(1 - \eta_{\text{o}}\right) + \frac{\eta_{\text{o}} T_{\text{air}} \left(\dfrac{1}{T_{\text{p}}} - \dfrac{1}{T_{\text{Sun}}}\right)}{\left(1 - \dfrac{T_{\text{air}}}{T_{\text{Sun}}}\right)} + \frac{U_l \left(T_{\text{p}} - T_{\text{air}}\right)\left(1 - \dfrac{T_{\text{air}}}{T_{\text{p}}}\right)}{I_T \left(1 - \dfrac{T_{\text{air}}}{T_{\text{Sun}}}\right)} + \right.$$
$$\left. + \frac{\dot{m} C_p T_{\text{air}} \left[\ln\left(\dfrac{T_{\text{out,cp}}}{T_{\text{in,cp}}}\right) - \left(\dfrac{T_{\text{out,cp}} - T_{\text{in,cp}}}{T_{\text{p}}}\right)\right]}{I_T A_{\text{p}} \left(1 - \dfrac{T_{\text{air}}}{T_{\text{Sun}}}\right)} \right\} \tag{28}$$

Water pipe

The hot water pipe of the collector is assumed to be a closed system for energy and exergy equilibrium analysis, with constant properties. The heat energy from collector plate is carried out by water flowing inside the pipe.

Energy absorption without insulation

The energy balance equation by considering the mass-flow inside the pipe, is given:

$$\dot{Q}_{\text{in,wp}} + \dot{m}\theta_{\text{in,wp}} = \dot{Q}_{\text{out,wp}} + \dot{m}\theta_{\text{out,wp}} \tag{29}$$

$$\dot{m}\theta_{\text{in,wp}} = \dot{m}_{\text{in}} \left(h_{\text{in}} + \frac{C_{\text{in}}^2}{2} + \text{g}Z_{\text{in}}\right)_{\text{wp}} \tag{30}$$

where θ is the energy associated with the flowing fluid, h – the the enthalpy, Z – the vertical height from the reference, g – the acceleration due to gravity, and C – the velocity of the fluid medium:

$$\dot{m}\theta_{\text{out,wp}} = \dot{m}_{\text{out}} \left(h_{\text{out}} + \frac{C_{\text{out}}^2}{2} + \text{g}Z_{\text{out}}\right)_{\text{wp}} \tag{31}$$

In the pipe flow, kinetic energy in and out, potential energy in and out are equal and can be neglected.

Energy absorption with insulation

The amount of heat loss is due to convection losses in the connecting pipes between the absorber plate and storage tank. Since the temperature of the fluid-flowing inside the pipes is higher than the surrounding temperature, there will be huge amount of heat loss to the surroundings. By selecting suitable insulating material for the connecting pipes, heat loss can be reduced. This reduces the exergy destruction and increases the Second law efficiency of the system to a limit. The proposed insulating material is glass wool in fig. 4 due to its low cost and good insulating properties. The energy balance for the insulated water pipe:

Figure 4. Insulation of pipes using glass wool

$$\dot{Q}_{\text{in,wp}} = \dot{m}\theta_{\text{out,wp}} - \dot{m}\theta_{\text{in,wp}} \tag{32}$$

Entropy generation

The heat loss rate in the water pipe without insulation is evaluated:

$$\dot{Q}_{l,\text{wp}} = \frac{L\pi\left(T_\text{f} - T_\text{air}\right)}{\dfrac{\ln\left(\dfrac{D_\text{o}}{D_i}\right)}{2k} + \dfrac{1}{h_\text{sf} D_\text{o}}} \tag{33}$$

The heat loss rate in the water pipe with insulation is evaluated:

$$\dot{Q}_{l,\text{wp}} = \frac{L\pi\left(T_\text{f} - T_\text{air}\right)}{\dfrac{\ln\left(\dfrac{D_\text{s}}{D_i}\right)}{2k} + \dfrac{1}{h_\text{sf} D_\text{s}}} \tag{34}$$

The rate of change of the entropy generated in the water pipe is given:

$$\dot{S}_{\text{gen,wp}} = \frac{\dot{Q}_{l,\text{wp}}}{T_\text{air}} \tag{35}$$

Storage tank

A storage tank in fig. 5 is the main component of the SWH to be considered for sizing. Principle of storage tank is to provide: Generous amount of hot water storage; a reasonable price to build, and a long boring life.

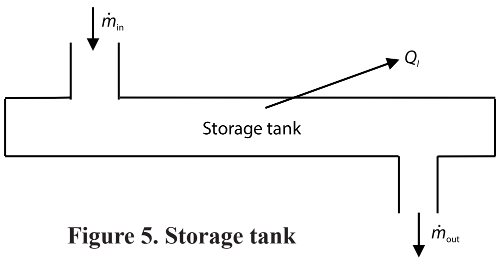

Figure 5. Storage tank

Energy absorption

The useful heat gain from storage tank to end user is expressed:

$$\dot{Q}_{\text{st}} = \dot{m}C_p\left(T_{\text{out,cp}} - T_{\text{t,st}}\right) \tag{36}$$

Entropy generation

The heat loss rate in the storage tank is evaluated:

$$\dot{Q}_{l,\text{st}} = \frac{\left(T_{\text{t,st}} - T_{\text{air}}\right)}{\left(\dfrac{1}{\pi h_{\text{sf}} D_{\text{st}} H_{\text{st}}}\right)} \tag{37}$$

where D_{st}, H_{st} is the diameter and height of the storage tank, respectively. The rate of change of entropy generated in the storage tank is given:

$$\dot{S}_{\text{gen,st}} = \frac{\dot{Q}_{l,\text{st}}}{T_{\text{air}}} \tag{38}$$

Exergy destruction and exergy efficiency

The exergy rate from collector plate to storage tank is calculated:

$$\dot{X}_{\text{cp,st}} = \dot{m}C_p\left(T_{\text{out,cp}} - T_{\text{t,st}}\right) - \dot{m}T_{\text{air}}C_p\ln\left(\frac{T_{\text{out,cp}}}{T_{\text{t,st}}}\right) \tag{39}$$

The exergy rate from storage tank to end user is given:

$$\dot{X}_{\text{st,end}} = \dot{m}C_p\left\{\left(\frac{T_{\text{t,cp}} + T_{\text{b,st}}}{2} - T_{\text{air}}\right) - T_{\text{air}}\left[\ln\left(\frac{T_{\text{t,st}}}{T_{\text{air}}}\right) - 1\right] - \frac{T_{\text{b,st}}T_{\text{air}}}{T_{\text{t,st}} - T_{\text{b,st}}}\ln\left(\frac{T_{\text{t,st}}}{T_{\text{b,st}}}\right)\right\} \tag{40}$$

where $T_{\text{b,st}}$ is the temperature of the water at bottom of the storage tank. The exergy destruction:

$$\dot{X}_{\text{des,st}} = T_o\dot{S}_{\text{gen,st}} \tag{41}$$

$$\eta_{\text{ex,st}} = 1 - \frac{\dot{X}_{\text{des,st}}}{\dot{X}_{\text{in,st}}} \tag{42}$$

Results and discussion

Table 1 represents the geometrical parameters of SWH and thermophysical properties of agent fluid. Assuming 1-D heat flow and considering the thermal capacity and temperature drop across the glass cover, iterative procedure was employed to estimate the top loss coefficient.

An extensive exergy analysis has been carried out in each subsystem of SWH. Exergy efficiency in tab. 2. is high for glass plate whereas for other subsystems it is drastically low, which makes a room for the researchers to examine modification in the system for the improvement in exergy efficiency.

Table 1. Environmental parameters and specifications of the SWH

SWH parameters	Values
Mass-flow rate of the working fluid, $\dot{m}$	0.002 kg/s
Heat capacity of the fluid, C_p	4186 kJ/kgK
Type	Black paint header-riser flat plate
Outlet temperature, T_{out}	360 K
Glazing	Double glass
Agent fluid in flow ducts	Water
Adhesive resistance	Negligible
Length and width of the collector	1.88 m × 0.98 m
Wind speed V_a	25 m/s
Collector tilt, β	20°
Fluid inlet temperature, T_{in}	305 K
Ambient temperature, T_{air}	300 K
Apparent Sun temperature, T_{Sun}	4350 K
Plate thickness, δ_{p}	0.002 m
Optical efficiency, $\eta_{\text{o}} = (\tau\alpha)$	0.84
Emissivity of the absorber plate, ε_{p}	0.92
Emissivity of the covers, ε_{c}	0.88
Glass covers distance, $\delta_1 = \delta_2$	0.04 m
Thickness of back insulation, δ_{b}	0.08 m
Thickness of sides insulation, δ_{e}	0.04 m
Thermal conductivity of the absorber plate, K_{p}	384 W/mK
Thermal conductivity of the insulation, K_{i}	0.05 W/mK
Incident solar energy per unit area of the absorber plate, I_T	500 W/mK
Tubes center to center distance, W	0.15 m
Inner diameter of the pipe, D_{i}	0.04 m
Outer diameter of the pipes, D_o	0.044 m
Fluid temperature at top of the storage tank, $T_{\text{t,st}}$	343 K
Fluid temperature at bottom of the storage tank, $T_{\text{b,st}}$	312 K
New outlet temperature of water from collector plate, $T_{\text{out,cp}}$	362 K
New fluid temperature at top of the storage tank, $T_{\text{t,st}}$	362 K
Diameter of the storage tank, D_{st}	1370 mm
Height of the storage tank, H_{st}	1465 mm
Length of the pipe, L	9 m

Table 2. Exergy analysis of the existing model

Components of SWH	Energy absorption, $\dot{Q}_{\text{abs}}$ [kW]	Entropy generation, $\dot{S}_{\text{gen}}$ [kWK^{-1}]	Exergy destruction, $\dot{X}_{\textbf{des}}$ [kW]	Exergy efficiency, η_{II} [%]
Glass plate	2.2599	0.646	0.193	92.101
Collector plate without honeycomb	0.461	$1.689 \cdot 10^{-3}$	0.504	5.181
Water pipes without insulation	0.0670	$2.612 \cdot 10^{-3}$	0.778	1.354
Storage tank	0.2595	0.01165	3.4726	1.280

To account the irreversibility in each subsystem, the present study customized a honeycomb structure placed between the glass and absorber plate to reduce the convective and radiation losses. It is observed that the exergy efficiency of collector plate has been slightly increased. However, the effects of honeycomb and pipe insulation are not showing much change in the exergy efficiency, but this change may conserve a lot of energy in the long run. Also, if there is any irreversibility in the system, it gets converted into useful work which leads to improvement of performance of the system. Table 3 shows the increase in the efficiency of each subsystem after converting the hidden losses into useful work.

Table 3. Exergy analysis of the modified model

Components of SWH	Energy absorption, $\dot{Q}_{abs}$ [kW]	Entropy generation, $\dot{S}_{gen}$ [kWK^{-1}]	Exergy destruction, $\dot{X}_{des}$ [kW]	Exergy efficiency, η_{II} [%]
Glass plate	2.2599	0.646	0.193	92.101
Collector plate with honeycomb	0.4772	$1.605 \cdot 10^{-3}$	0.478	5.298
Water pipes with insulation	0.0921	$5.861 \cdot 10^{-4}$	0.175	1.914
Storage tank	0.2763	0.0112	3.3243	1.832

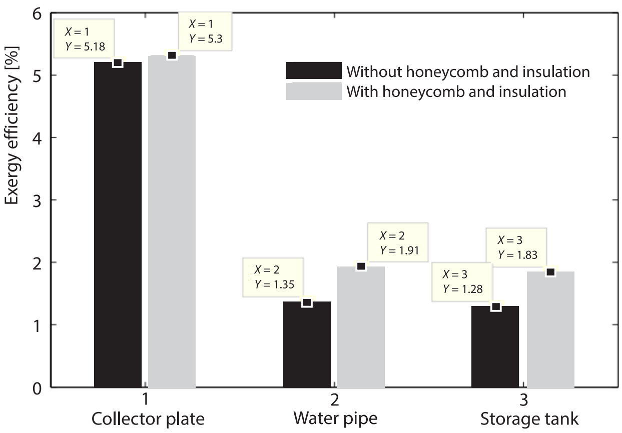

Figure 6. The variations of exergy efficiency between existing model and modified model

With the help of exergy analysis, the energy input and output are equated which gives a clear picture of the system, including hidden losses. The Second law efficiency has been analyzed before and after the improvisation of energy efficiency. Figure 6 illustrates that by reducing the losses in each subsystem, the exergy efficiency of the collector plate, water pipe and storage tank are increased from 5.181-5.298%, 1.354-1.914%, and 1.280-1.832%, respectively.

Figure 7(a) shows that the exergy efficiency and the collector plate area are positively correlated up to a maximun point for both the models, then the efficiency between the models coincides. Figure 7(b) demonstrates the increase in exergy efficiency progressively up to a specified inlet temperature and its decrease as inlet temperature increases. Thus, the exergy efficiency of the system is optimum up to a particular fluid temperature.

Figures 8(a) and 8(b) illustrates the variations of exergy efficiency as a function of collector plate area and mass-flow rate of the agent fluid in 3-D views. It is inferred that the exergy efficiency is maximum at fixed lower flow rate for the range of collector plate area. This is due to the effective transformation of energy from the collector plate to the agent fluid. The efficiency decreases gradually when the flow rate of the fluid is increased for the range of collector plate area.

Figure 9(a) points that the exergy efficiency increases as the optical efficiency increases and the difference between the exergy efficiency of both the models are consistent with increase in optical efficiency. Figure 9(b) shows the effect of incident solar energy per unit area

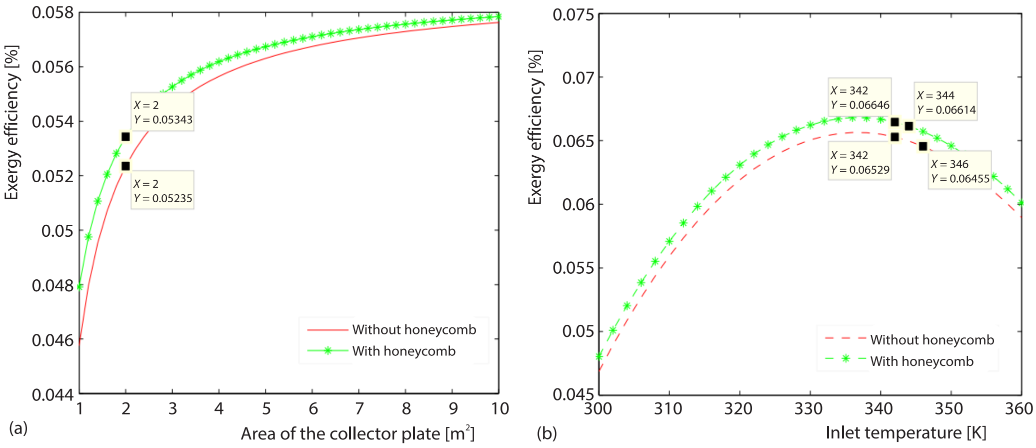

Figure 7. (a) Area of the plate *vs.* exergy efficiency and (b) inlet temperature *vs.* exergy efficiency

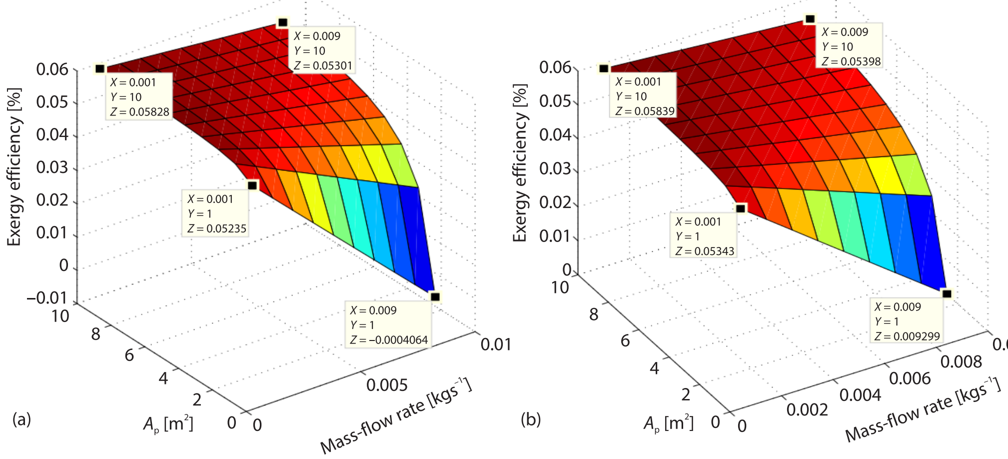

Figure 8. Variations of exergy efficiency according to mass-flow rate and area of the plate; (a) for the existing model and (b) for the modified model

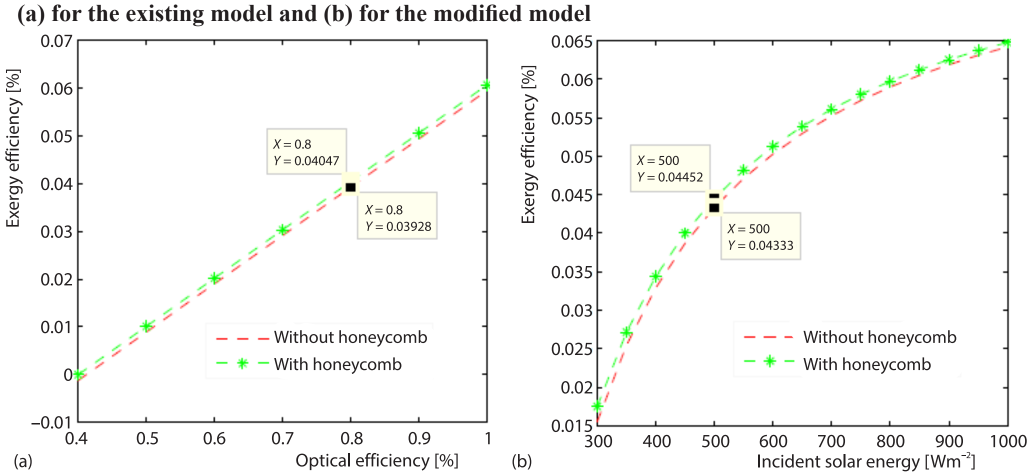

Figure 9. (a) Exergy efficiency *vs.* optial efficiency and (b) exergy efficiency *vs.* incident solar energy per unit area of the flat plate collector

of the flat plate collector and exergy efficiency increases with respect to this parameter and the variation between the exergy efficiency of the existing model and modified model is reduced with increase in incident soalr energy.

Conclusion and future scope

In this work, a SWH with flat plate collector was experimentally tested: with and without honeycomb structure inserted between glass plate and collector plate and with and without insulated water pipe.

Based on this study the following conclusions have been drawn as follows.

- Exergy efficiencies for the consecutive stages of solar water heater are calculated and the results of the entropy generation and exergy destruction are compared with both existing and modified model. The obtained results showed that the accuracy of the exergy efficiency of the collector plate, water pipe and storage tank are increased from 5.181-5.298%, 1.354-1.914%, and 1.280-1.832%, respectively. Though the impact of honeycomb structure and water pipe insulation is showing feeble variation in the exergy efficiency, this change may eventually preserve a lot of energy.
- The graphical results showed that the exergy efficiency and the collector plate area are positively correlated. Also, increase in fluid inlet temperature, increases exergy efficiency up to a maximum point, beyond which they are negatively correlated. By increasing the optical efficiency, exergy efficiency increases and varies uniformly for both the models. Moreover, the obtained results showed a positive correlation between exergy efficiency and incident solar energy per unit area of the flat plate collector.
- The exergy analysis presented in this paper can be extended to introduce the phase change material module of similar system, to establish the analysis of hidden losses. The future scope of the work is to carry out an exergoeconomic analysis to bring out the exergy cost which is useful for performing thermal analysis of any system.
- This study concludes that any product which comes out through an exergy analysis designates the conservation of energy to a greater extent which may support the energy demand for future generation.

Nomenclature

A – area, [m^2]
C_p – heat capacity, [kJkg^{-1}K^{-1}]
D – diameter, [m]
D_s – outside diameter of the pipe, [m]
d – depth of the honeycomb, [m]
F' – collector efficiency factor, [–]
F_R – heat removal factor, [–]
G_{solar} – total solar irradiation, [–]
h – heat transfer coefficient, [Wm^{-2}K^{-1}]
I_T – incident solar energy per unit area of the absorber plate, [Wm^{-2}]
K – thermal conductivity, [Wm^{-1}K^{-1}]
L – dimensions of the plate, [m]
$\dot{m}$ – mass-flow rate, [kgs^{-1}]
$\dot{Q}$ – heat energy rate, [kW]
$\dot{S}$ – entropy rate, [kWK^{-1}]
S_r – radiation absorbed flux per unit area of absorber plate, [Wm^{-2}]
T – temperature, [K]
W – pitch of the tube, [m]
w – honeycomb cell width, [m]
$\dot{X}$ – exergy rate, [kW]
Z – vertical height from the reference, [m]

Greek symbols

α_s – solar absorptivity
β – collector tilt
δ – thickness
ε – emissivity
η – efficiency
σ – Stefan-Boltzmann constant
$\tau\alpha$ – effective product transmittance-absorptance

Subscripts

abs – absorbed
air – ambient
b – bottom

cp – collector plate
conv – convective
des – destruction
ex – exergy
f – fluid
gen – generated
gp – glass plate
hc – honeycomb
in – input
l – loss
lk – leaked
o – outer
out – output
p – plate
s – surface
sf – surface
sd – stored
st – storage tank
t – top
wp – water pipe

References

[1] Suzuki, A., A Fundamental Equation for Exergy Balance on Solar Collectors, *Journal Sol. Energy Eng., 110* (1988), 2, pp. 102-106
[2] Gupta, D. K. K., Saha, S. K., Energy Analysis of Solar Thermal Collectors, *Journal Renew. Energy & Environ.,* (1990), pp. 283-287
[3] Luminosu, I., Fara, L., Determination of the Optimal Operation Mode of a Flat Solar Collector by Exergetic Analysis and Numerical Simulation, *Energy*, *30* (2005), 5, pp. 731-747
[4] Farahat, S., *et al*., Exergetic Optimization of Flat Plate Solar Collectors, *Renew. Energy*, *34* (2009), 4, pp. 1169-1174
[5] Jafarkazemi, F., *et al*., Energy and Exergy Efficiency of Heat Pipe Evacuated Tube Solar Collectors, *Thermal Science, 20* (2016), 1, pp. 327-335
[6] Zhong, G., *et al*., Exergy Analysis of Flat Plate Solar Collectors. *Entropy*, *16* (2014), 5, pp. 2549-2567
[7] Sivaraman, G., *et al*., Experimental Investigation on Effect of Modified Solar Collector in Solar Water Heating System, *Thermal Science, 24* (2020), 1, pp. 481-485
[8] Malvi, C. S., *et al*., Experimental Investigation of Heat Removal Factor in Solar Flat Plate Collector for Various Flow Configurations, *Int. J. Green Energy*, *14* (2017), 4, pp. 442-448
[9] Orlando, M. M., Jose, J. F. P., Heat Removal Factor in Flat Plate Solar Collectors: Indoor Test Method, *Energies*, *11* (2018), 10, 2783
[10] Hollands, K. G. T., Honeycomb Devices in Flat Plate Solar Collectors, *Proceedings*, Solar Energy Society Conference, Phoenix, Ariz., USA, 1965, Vol. 9, pp. 159-164
[11] Mozumder, A., *et al*., Study of Cylindrical Honeycomb Solar Collector, *Journal Sol. Energy, 2014* (2014), ID 539894
[12] Abdullah, A, H., Thermal Performance of Flat Plate Solar Collector using Various Arrangements of Compound Honeycomb, *Energy Convers. Manag., 44* (2003), 19, pp. 3093-3112
[13] Dincer, I., Cengel, Y. A., Energy, Entropy and Exergy Concepts and Their Roles in Thermal Engineering, *Entropy*, *3* (2001), 3, pp. 116-149
[14] Hottel, H. C., Keller, J. D., Effect of Reradiation on Heat Transmission in Furnaces and Through Openings, *Trans. ASME, 55* (1933), 55-56, pp. 39-49
[15] Sukhatme, S. P., *Solar Energy,* McGraw-Hill., New York, USA, 2014
[16] Najian, M. R., Exergy Analysis of Flat Plate Solar Collector, Mc. S. thesis, Tehran University, Tehran, Iran, 2000

Paper submitted: May 30, 2020
Paper revised: October 28, 2020
Paper accepted: November 12, 2020